FE-2727-6
Distribution Category UC-90d

MASS TRANSPORT CHARACTERISTICS OF ZEOLITE CRACKING CATALYSTS

Quarterly Report for the Period
January 1-March 31, 1979

Henry W. Haynes, Jr.

The University of Mississippi
Department of Chemical Engineering
University, Mississippi 38677

Date Submitted - May 14, 1979

PREPARED FOR THE UNITED STATES
DEPARTMENT OF ENERGY

Under Contract No. EF-77-S-01-2727

MASS TRANSPORT CHARACTERISTICS OF ZEOLITE CRACKING CATALYSTS (FE-2727-6)

ABSTRACT

An active zeolite hydrocracking catalyst has been prepared by ion exchanging Ni^{++} onto an ammonium ultrastable zeolite Y and then impregnating the resulting catalyst with tungsten. A mixture of hydrogenated phenanthrenes were hydrocracked over this catalyst in a trickle bed reactor over a range of conditions: P = 1500-2000 psi, T = 650-750°F, SV = 0.5-3.0 gm/hr/gm. Operability was generally good for the entire 131 hour run duration. The products will be analyzed by gas chromatography with selected products analyzed by GC/MS.

A kinetics model has been developed for the simulated catalytic cracking of various pure hydrocarbons over zeolite NaY. Over the range of concentrations studied, hydrogenation prevails over cracking for partially saturated species like tetralin. The opposite is true for totally saturated naphthenic species such as decalin. However, the kinetic model predicts a higher selectivity toward cracking in a 100% vapor phase (no carrier gas) environment at atmospheric pressure. Tests are underway to check this prediction experimentally. From the magnitude of the activation energies and the relative activities for conversion over NaA and NaY, there does not appear to be any evidence of a pore diffusion limitation for the 3-ring and smaller components studie . (This conclusion may not apply to conventional catalytic cracking processes, however, since the conversion rates over NaY are orders of magnitude smaller than rates over acid forms of the zeolite.)

Unexplained discrepancies still exist between theory and experiment in the GC-diffusivity studies on the system n-butane/NaY. Further tests are planned to check the linearity assumptions inherent in the model.

OBJECTIVES AND SCOPE OF WORK

One objective of this program is to assess the significance of intracrystalline pore diffusion limitations when processing coal-derived syncrudes over zeolite cracking catalysts. The experimental work will involve parallel determinations of mass transport characteristics and catalyst activities using model coal-liquid compounds. A second objective will be to test various zeolite catalysts for their ability to crack coal-derived syncrudes to naphtha.

The purpose of task 1 is to identify the range of critical molecular diameters corresponding to the point at which entrance to sodium zeolite Y crystallites becomes severely restricted at near reaction conditions. In task 2 we will establish the extent to which hydrothermal treatment may affect the intracrystalline diffusivities of high molecular weight hydrocarbons in the hydrogen form of zeolite Y, and the effect of chemical dealumination will be established in task 3. The purpose of task 4 is to test selected zeolite catalysts for their activities and selectivities in cracking model coal-liquid compounds and fractions of coal-derived syncrudes to naphtha under conditions which simulate catalytic cracking. Hydrocracking tests on zeolite-containing catalysts will be conducted in task 5.

SUMMARY OF PROGRESS TO DATE

The chart on the next page summarizes the progress to date. The simulated hydrocracking studies appear to be well on schedule. We are behind in the simulated catalytic cracking studies, but we are well into our studies with the hydrothermally treated NH_4Y zeolite (ultrastable zeolite). The GC diffusivity studies are lagging behind because of a thus far unexplained inability of the linear chromatography model to fit the data to the desired accuracy. We are hopeful that an explanation can be found soon and studies with other hydrocarbons can be resumed.

PROJECT PLAN AND PROGRESS REPORT AS OF 3/30/79

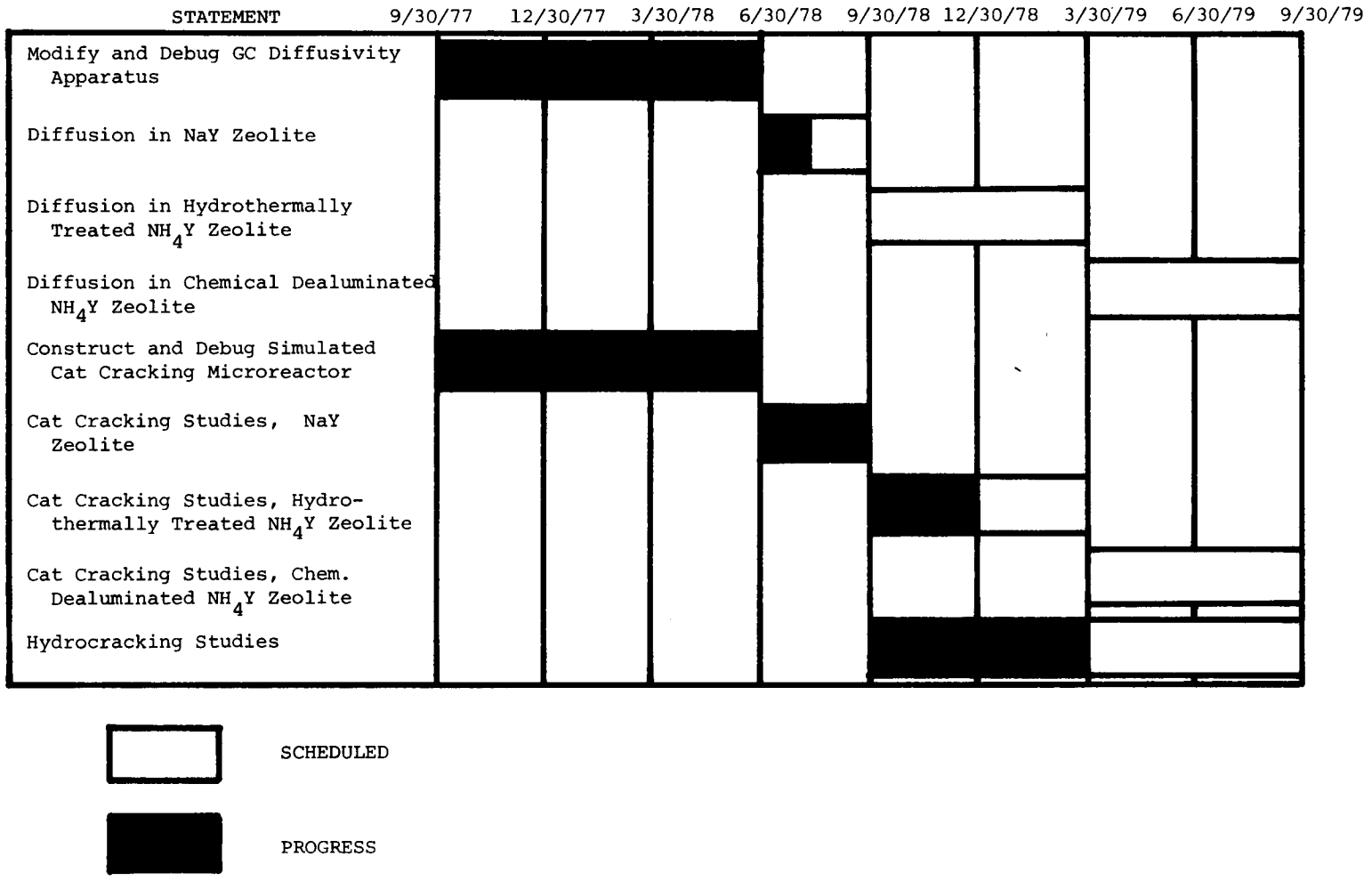

DETAILED DESCRIPTION OF TECHNICAL PROGRESS

Modifications to the hydrocracking apparatus are complete, a very active hydrocracking catalyst has been prepared, and a series of experiments using hydrogenated phenanthrenes as the feedstock have been completed (task 5). Kinetics of the catalytic cracking of various multiring species over zeolite NaY are detailed in this report (task 4). Additional GC-diffusivity studies on the system n-butane/zeolite NaY have only partly explained the discrepancies between theory and experiment noted in previous reports (task 1). These three items are discussed in more detail below.

Task 1 - Diffusion Studies in Zeolite NaY - H. W. Haynes, Jr. and Ling-Kai Paul Hsu

The system n-butane/zeolite NaY was investigated further during the last quarter in an attempt to explain the differences between the theory and experiment that were noted in the previous report (1). In the previous report it was postulated that these differences may be due in part at least to failure of the axial dispersion model in beds of small particles at high velocities. In order to test this hypothesis a series of experiments was completed at low velocities well into the molecular dispersion region. A discrepancy between theory and experiment was still evident. This test is not conclusive, however, since a larger input pulse size had to be used in order to achieve the required sensitivity in the output signal. (No tests for linearity have been undertaken with the larger sample loop; hence, the observed discrepancies could be due to system nonlinearities.)

Several other attempts to explain the differences between theory and experiment in the n-butane/NaY system met with failure. Inclusion of additional parameters, e.g. finite rate of adsorption, finite rate of external mass transfer, into the model were not successful. One revision in the model which gave somewhat improved results was a modification to take into account the distribution of crystallite sizes. A very efficient numerical means of integration over the particle size distribution was tested successfully. The particle size distribution for our zeolite sample was graciously determined by Dr. M.P. Mathur of the Pittsburgh Energy Research Center of DOE using a video microscopy technique. Not only did this modification give an improved fit, but the calculated diffusivities are about two orders of magnitude greater than those obtained on the basis of a mean particle size.

Despite this improvement, significant differences still exist between calculated and experimental response curves for the n-butane/NaY system. We have discounted system nonlinearities on the basis of our studies of the effect of pulse concentration on the observed response curve. Seeing no effect, we have assumed that the system is linear. [See Fig. 5.6 of our previous report (1).] However, it may be that

the pulse concentration was not varied over a wide enough range, or that the temperatures where this study was made were sufficiently high that the contributions from the mass transfer terms were too small to observe nonlinear effects. Ruthven reports that diffusion of n-butane in zeolite 13X is nonlinear even in the Henry's law region (2). Cerro and Smith have suggested that a localized heat effect may be responsible for failure of the linear chromatography theory to fit data for n-butane adsorption on silica gel (3). Additional tests are therefore needed to establish the linearity of the system in view of the important influence that nonlinearities can be expected to have on the results.

Work Forecast:

An injection port and dispersion tube are presently being installed just upstream of the inlet splitting tee. This modification will provide an alternative to the sample valve method of injection. With the new arrangement the effect of concentration can be determined quickly and simply by varying the injection volume. By providing a dispersed pulse the column inlet is not exposed to pure hydrocarbon as it is with the normal sample valve injection method. The pulse component can be varied conveniently without disturbing the column, and since very small quantities of hydrocarbon are needed a wider range of components can be studied.

With the completion of this modification, a new batch of catalyst will be prepared and further experiments with n-butane will be undertaken to check for system nonlinearities. Preliminary tests with other diffusing components, e.g. cyclohexane, will also be conducted during the next quarter.

Task 4 - Construct and Debug Simulated Catalytic Cracking Microreactor -

C. Z. Wan

The experimental parts of catalytic cracking of partially hydrogenated fused-ring compounds over NaY zeolite were discussed in previous reports (1,4); only the analysis of the kinetics will be detailed in this report. In the meantime, we have started our investigation of catalytic cracking of partially hydrogenated fused-ring compounds over USY zeolite and the results will be presented in the next report.

I. Catalytic Cracking over NaY Zeolite

Coke Formation and Reaction Path. As shown in Fig. 6.1, the determination of coke level at different accumulated times on stream (indicated above each experimental point) reveals that the quantity of coke formed on the NaY catalyst was not great. Most of the coke formed is due to the reaction within the initial twenty minutes time-on-stream. The activity

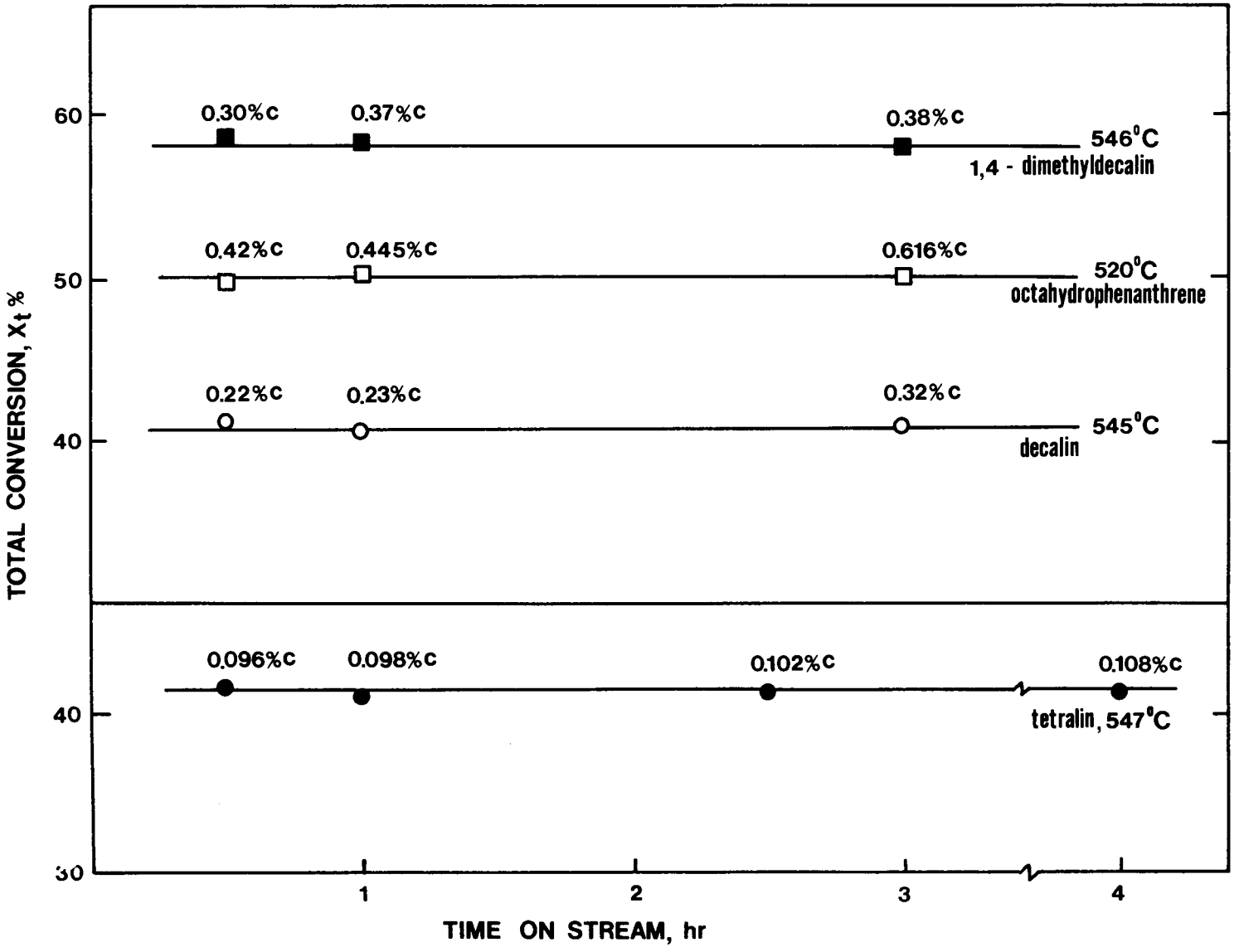

Fig. 6.1. *Catalyst Activity as a Function of Time on Stream Catalyst Weight 0.31 g. (a) For Tetralin and Decalin, Carrier Flow (Helium) 5.0 cc/min STP, Feed Rate, 0.115 cc/hr. (b) For 1,4 Dimethyldecalin, Carrier Flow 9.5 cc/min STP, Feed Rate 0.225 cc/hr. (c) For Octahydrophenanthrene, Carrier Flow 19.5 cc/min STP, Feed Rate 0.44 cc/hr.*

of the catalyst does not vary as the time-on-stream is increased up to four hours (~HC/cat. = 1.5 for tetralin and decalin, 3.0 for 1,4 dimethyl-decalin and 6.0 for octahydrophenanthrene) nor is it sensitive to the coke formation. Therefore, the analysis of the kinetics can be made in the steady state operation in our experiments.

Through experiments, the total conversion of polycyclic compounds and product compositions for cracking over NaY catalyst indicates the presence of at least two types of reaction paths. The first path which involves α-ring opening, followed by side chain cracking or isomerization contributes to the "cracking conversion". By another path the reactant undergoes dehydrogenation within the saturated fused-ring without involving any carbon-carbon bond scission. Conversion by this path is referred to as "dehydrogenation conversion". The reaction kinetics in this case may be expressed by the equation:

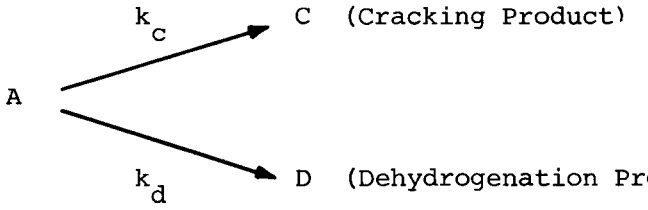

(4.1)

and

$$r = k_c C_A^{\alpha} + k_d C_A^{\beta} \tag{4.2}$$

The catalytic cracking of petroleum syncrude over zeolite catalysts has been reported to follow first order kinetics (5,6). Therefore, it is reasonable to assume $\alpha = 1$. Then, for a plug flow reactor, initial concentration of the reactant can be correlated with total conversion and parameter β.

$$\frac{W}{F} = \int_0^{X_t} \frac{d\,X_t}{k_c C_A + k_d C_B^{\beta}} \tag{4.3}$$

where W is the weight of catalyst, F is the feed rate, X_t is the total conversion, C_A° is the initial concentration of reactant, and $\dot{V}$ is the volumetric flow rate, or

$$(\beta-1)\,\frac{W}{\dot{V}} = \frac{1}{k_c}\,\ell n\,\frac{k_c(1-X_t)^{1-\beta} + k_d\,C_A^{\circ(\beta-1)}}{k_c + k_d\,C_A^{\circ(\beta-1)}} \tag{4.4}$$

or

$$C_A^{\circ(\beta-1)} \left[e^{\frac{W}{\dot{V}}(\beta-1)} - 1\right] \left(\frac{k_d}{k_c}\right) + e^{\frac{W}{\dot{V}}(\beta-1)} = (1-X_t)^{1-\beta} \tag{4.5}$$

Therefore, a plot of $C_A^{\circ(\beta-1)}$ vs. $(1-X_t)^{1-\beta}$ will verify the reaction kinetics for a given temperature and contact time. A typical example is shown in Fig. 6.2 where it is assumed that $\beta=0$. In the figure, carrier gas flow rate is kept constant, the variation of feed rate is equivalent to a change of initial concentration. This figure shows that the reaction of polycyclic compounds over NaY can be best described by a first order kinetics in cracking conversion and a parallel zero order kinetics in dehydrogenation conversion.

In such circumstances, an additional correlation between initial concentration and dehydrogenation conversion can be derived from the selectivity equation.

$$\frac{r_c}{r_d} = \frac{k_c C_A^{\circ} (1-X_t)}{k_d} \tag{4.6}$$

$$\frac{r_t}{r_d} = \frac{k_c C_A^{\circ} (1-X_t) + k_d}{k_d} = \frac{dX_t}{dX_d} \tag{4.7}$$

or

$$\int_0^{X_d} \frac{dX_d}{k_d} = \int_0^{X_t} \frac{dX_t}{k_c C_A^{\circ} (1-X_t) + k_d} = \frac{W}{F} \tag{4.8}$$

or

$$X_d = \left(\frac{k_d \cdot W}{C_A^{\circ}}\right) \cdot \left(\frac{1}{\dot{V}}\right) \tag{4.9}$$

Consequently, a plot of X_d vs contact time should give a straight line for a constant initial concentration. Figure 6.3 shows a typical example.

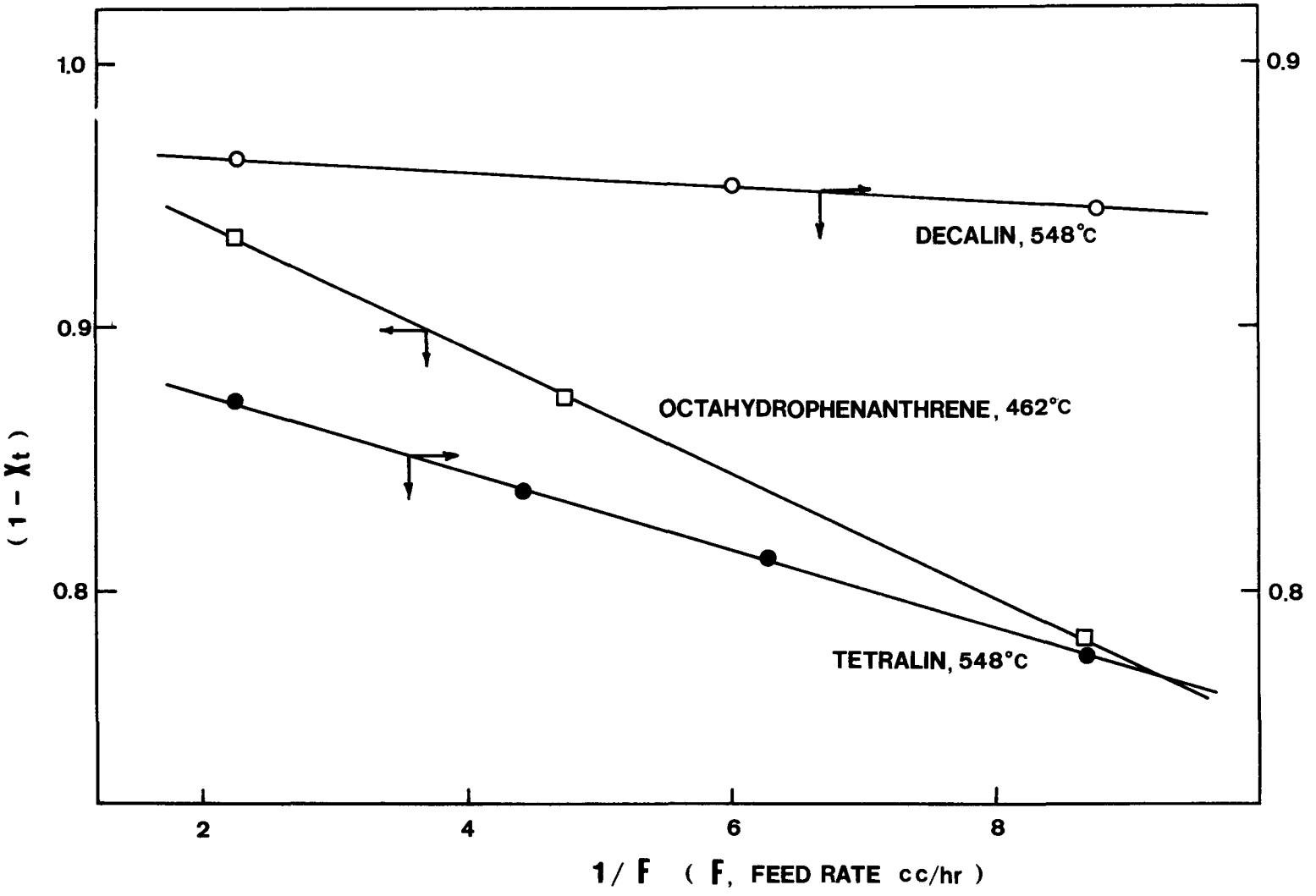

Fig. 6.2. *Total Conversion as a Function of Feed Rate. Catalyst Weight 0.31g, Carrier Flow 19.5 cc/min STP.*

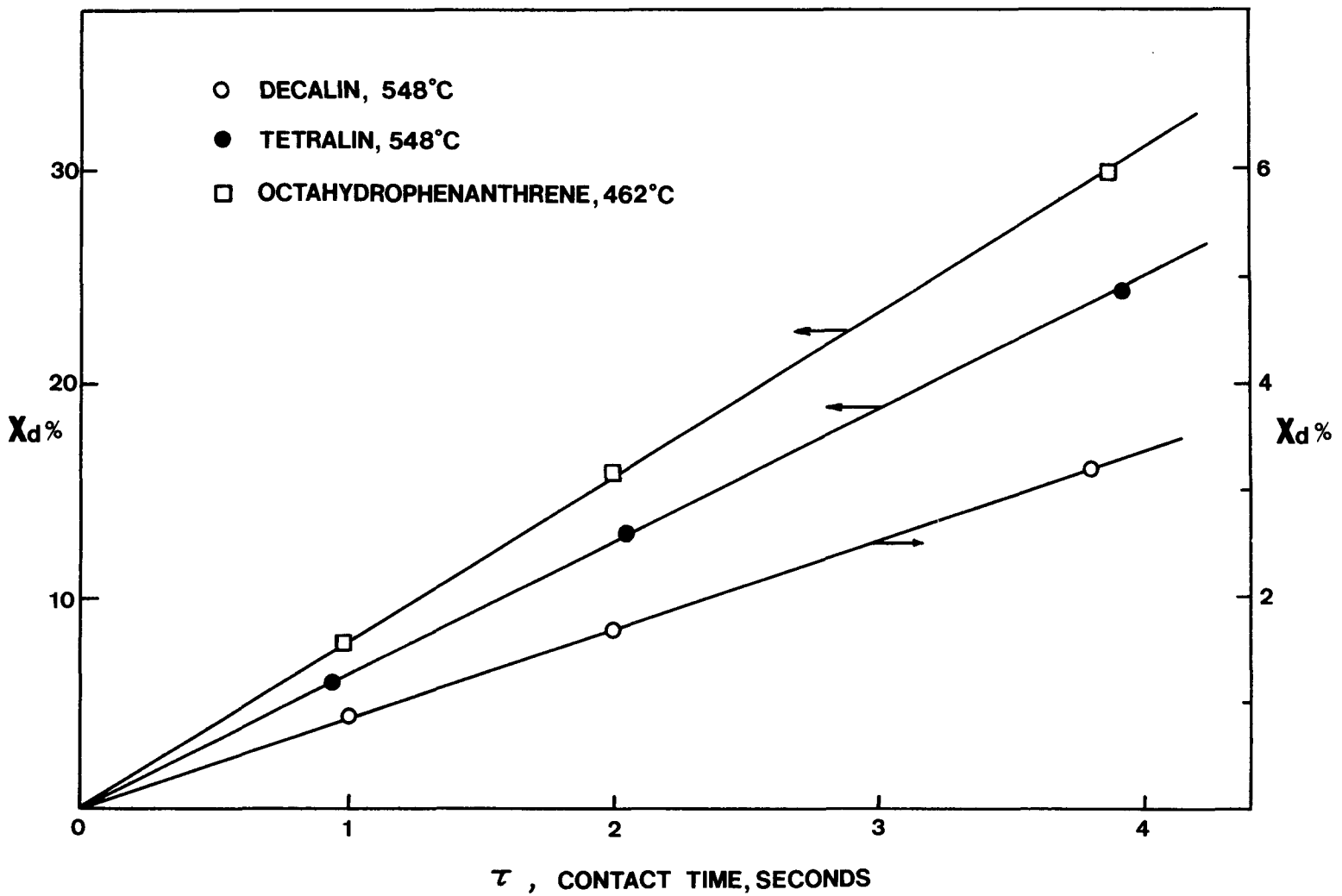

Fig. 6.3. *Dehydrogenation Conversion as a Function of Contact Time. Catalyst Weight 0.31 g, C_A° in Vol % Vapor at STP, 6.0% for Tetralin, 5.2% for Decalin, 4.4% for Octahydrophenanthrene.*

Then, the apparent rate constants can be calculated from the slopes of these straight lines.

Figures 6.4 and 6.5 present typical Arrhenius plots of dehydrogenation rate constant and cracking rate constant respectively. With each compound, the good linear plot gives the activation energies for dehydrogenation conversion and cracking conversion. It is interesting to note that activation energies for dehydrogenation conversion for most of the two fused-ring compounds we studied are about 50 kcal/mole. In another respect, the activation energies for cracking conversion show the trend of higher values for saturated compounds than for partially hydrogenated compounds and vary from 40 to about 60 kcal/mole. The Arrhenius plot for three-fused ring compound (e.g. octahydrophenanthrene) shows that activation energy for cracking conversion remains constant about 57 kcal/mole over wide range of temperature. However, activation energy for dehydrogenation conversion decreases gradually as temperature increases above 500°C as shown in Fig. 6.6. This may be due to a desorption control mechanism for dehydrogenation conversion. In such circumstances, the surface concentration of reactant decreases as temperature increases and finally results in a decrease in desorption rate. The rate constants for some fused-ring compounds cracking over NaY and NaA as a function of temperature are collected in Table 6.1. Table 6.2 compares relative rates with the two catalysts for fused-ring hydrocarbons with increasing number of rings per molecule. It shows that the overall rates of reaction of fused ring compounds over NaA increase with the increase in molecular size. The critical diameters of the fused-ring compounds of interest are somewhat greater that 6 Å. Therefore they will not enter the NaA zeolite crystallite which will reflect the fraction of contribution of the reaction over the outside surface of NaY zeolite because NaY and NaA are very similar in chemical nature. It is interesting to note that the multi-fused ring compounds have lower reaction rates than single fused-ring compounds (e.g. n-butylbenzene) in NaY crystallite. However, the increasing ratio of rate constants for multi-fused ring compounds indicates that the mass transfer limitation of octahydrophenanthrene (critical diameter 8.0 Å) or 1,4 dimethyldecalin (critical diameter 8.4 Å) cracking over NaY if it does exist will be rather small. In another respect, the high activation energies for both cracking and dehydrogenation conversion (>40 kcal/mole) and also invariant reaction order over wide range of temperature indicate that the reaction of fused-ring compounds we have studied are kinetically controlled. Therefore, it is reasonable to conclude that the mass transfer limitation of fused-ring compounds with molecular size up to 8.4 Å is insignificant when these compounds are processed over NaY zeolite in a temperature below 1000°F.

Product Distribution. In the previous section, we have discussed the reaction kinetics of catalytic cracking of fused-ring compounds over NaY. In this section, we would like to discuss the selectivity of the reaction over NaY. We will start from the selectivity equation

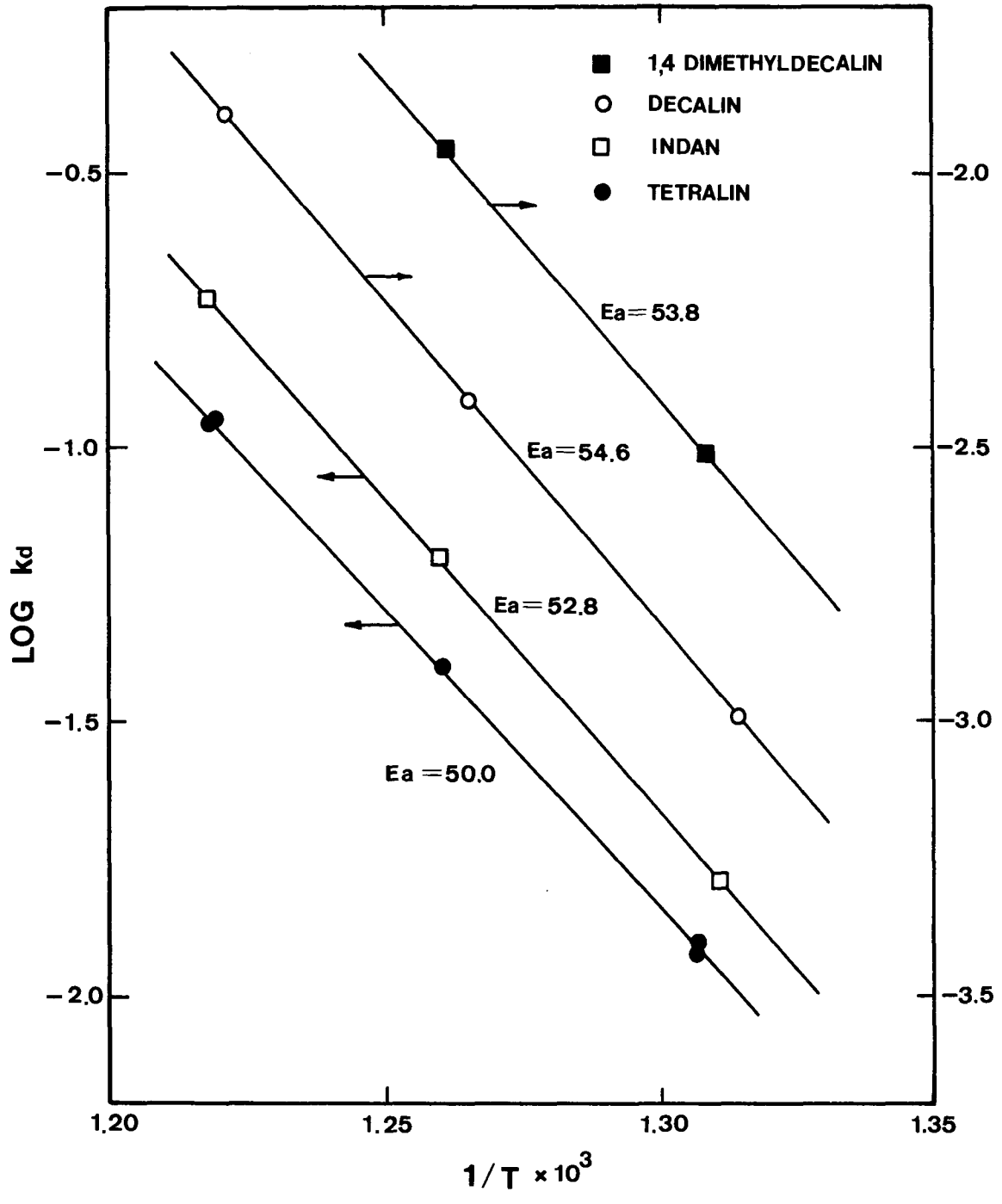

Fig. 6.4. *Dehydrogenation Conversion Rate Constant k_d as a Function of Temperature [k_d in g/(g-cat)(hr)].*

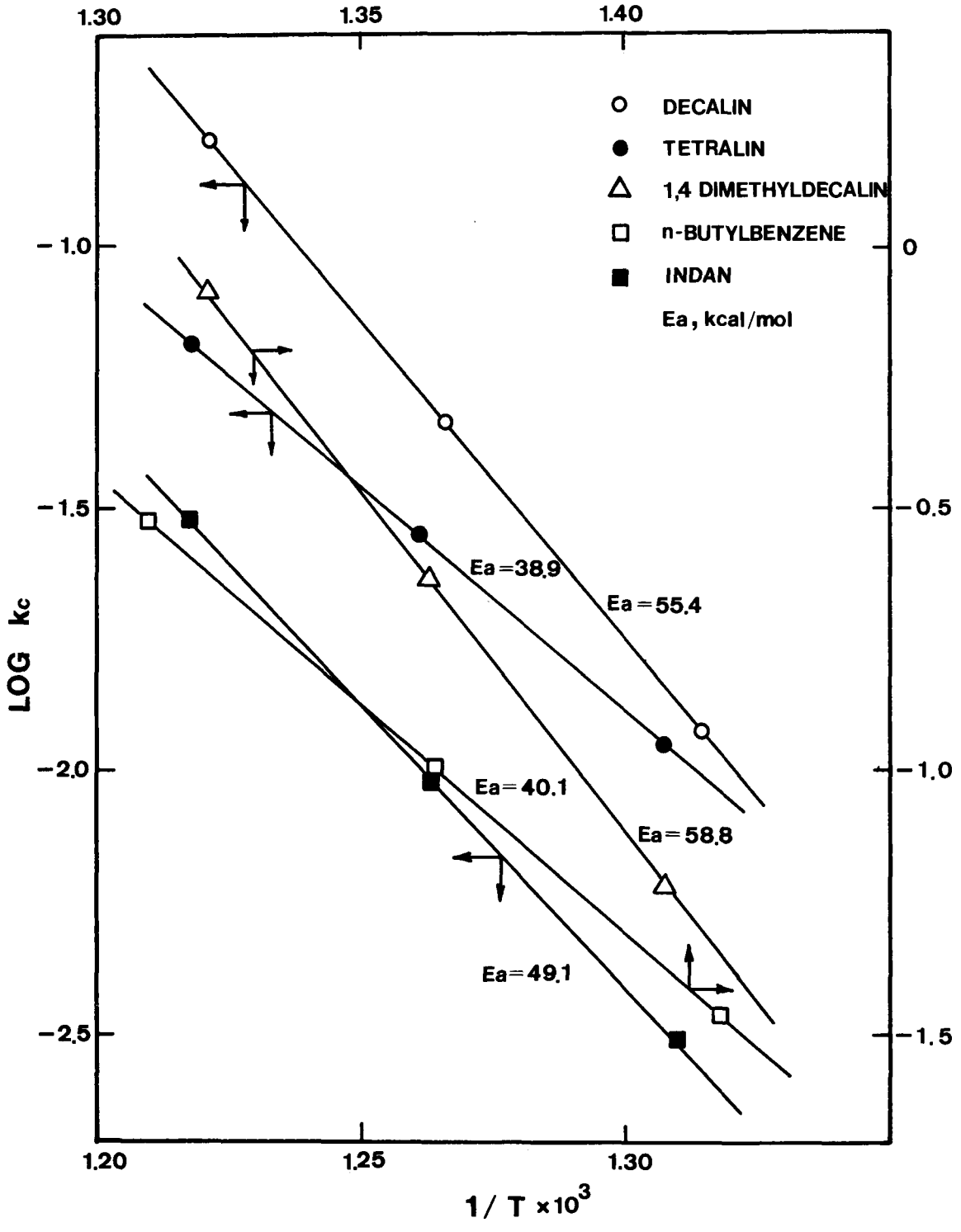

Fig. 6.5. *Cracking Conversion Rate Constant k'_C as a Function of Temperature [$k'_C = (k_C)\ C^\circ_A$, g/(g-cat)(hr)].*

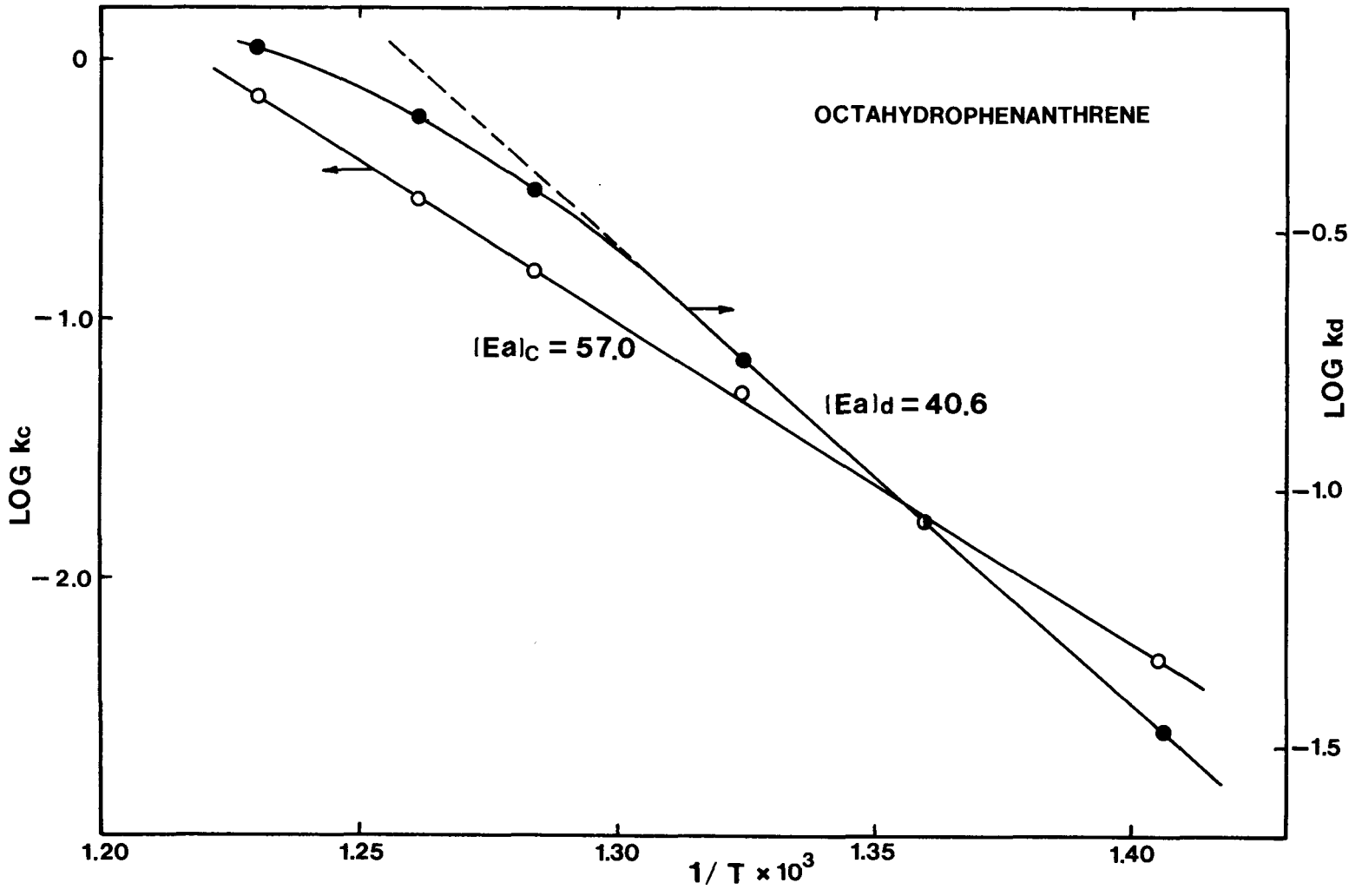

Fig. 6.6. *Dehydrogenation Rate Constant k_d and Cracking Rate Constant k_c' as a Function of Temperature for Octahydrophenanthrene (Ea, kcal/mole).*

Table 6.1

Summary of rate constants for some fused-ring compounds cracking over NaY and NaA

Fused Ring Compounds	NaY	NaA
	Dehydrogenation k_d, g/(g-cat.)(hr)	
n-butylbenzene	-	-
tetralin	$2.38 \times 10^{12} \exp(-\frac{25,160}{T})$	$2.24 \times 10^{11} \exp(-\frac{24,860}{T})$
decalin	$4.945 \times 10^{12} \exp(-\frac{27,480}{T})$	$1.53 \times 10^{11} \exp(-\frac{26,070}{T})$
1,4 dimethyl-decalin	$5.287 \times 10^{12} \exp(-\frac{27,080}{T})$	$3.457 \times 10^{11} \exp(-\frac{26,170}{T})$
octahydrophenanthrene	$1.0 \times 10^{11} \exp(-\frac{20,430}{T})$	$1.646 \times 10^{8} \exp(-\frac{17,970}{T})$
	($T < 500°C$)	
	Cracking $k_c C_A^\circ$, g/(g-cat.)(hr)	
n-butylbenzene	$9.34 \times 10^{10} \exp(-\frac{20,180}{T})$	$4.58 \times 10^{8} \exp(-\frac{20,130}{T})$
tetralin	$1.44 \times 10^{9} \exp(-\frac{19,580}{T})$	$2.19 \times 10^{7} \exp(-\frac{18,570}{T})$
decalin	$9.89 \times 10^{13} \exp(-\frac{27,880}{T})$	$2.314 \times 10^{11} \exp(-\frac{25,920}{T})$
1,4 dimethyl-decalin	$2.928 \times 10^{15} \exp(-\frac{29,590}{T})$	$9.30 \times 10^{11} \exp(-\frac{26,170}{T})$
octahydrophenanthrene	$1.47 \times 10^{15} \exp(-\frac{28,690}{T})$	$1.90 \times 10^{6} \exp(-\frac{16,100}{T})$

Table 6.2

Relative rate constants at 520°C

Fused Ring Compounds	Overall rate over NaA k, g/(g-cat.)(hr)
n-butylbenzene	4.325×10^{-3}
tetralin	6.433×10^{-3}
octahydrophenanthrene	2.67×10^{-2}
decalin	2.13×10^{-3}
1,4 dimethyldecalin	5.94×10^{-3}
	Cracking k_{NaY}/k_{NaA}
n-butylbenzene	191.5
tetralin	28.2
decalin	33.5
1,4 dimethyldecalin	39.4
octahydrophenanthrene	99.6
	Dehydrogenation k_{NaY}/k_{NaA}
tetralin	7.3
decalin	4.9
1,4 dimethyldecalin	4.9
octahydrophenanthrene	21.8

$$\int_0^{X_d} \frac{dX_d}{k_d} = \int_0^{X_t} \frac{dX_t}{k_c C_A^\circ (1-X_t) + k_d} \tag{4.8}$$

or

$$\frac{X_d}{k_d} = \frac{1}{k_c C_A^\circ} \ln \frac{k_c C_A^\circ + k_d}{k_c C_A^\circ (1-X_t) + k_d} \tag{4.9}$$

therefore

$$a X_d = - \ln (1 - b X_t) \tag{4.10}$$

where

$$a = \frac{k_c C_A^\circ}{k_d} \quad , \quad b = \frac{k_c C_A^\circ}{k_c C_A^\circ + k_d}$$

and

$$X_t = X_c + X_d \tag{4.11}$$

For a given temperature and initial concentration of the reactant, a selectivity plot between X_d and X_t can be made. Figure 6.7 to Figure 6.9 present the selectivity plots for double fused-ring compounds, tetralin (5.945 vol% in vapor at STP), indan (6.551%) and decalin (5.216%) respectively. In these plots, the lines are calculated values, dots are experimental points. They are shown to be in excellent agreement. The selectivity plot for tetralin is a function of temperature because the activation energies for cracking and dehydrogenation conversion are different. In the case of no appreciable difference in values of activation energies between cracking and dehydrogenation conversion, the selectivity plot will be independent of temperature. The reaction of indan and decalin are examples of the latter case. From the selectivity plots, we can see that in the case of partially hydrogenated compounds (such as tetralin, indan, etc.) dehydrogenation dominates the product distribution at high temperature and high conversion. However, in the catalytic cracking of completely hydrogenated fused-ring compounds, (such as decalin, 1,4 dimethyldecalin) dehydrogenation makes only a minor contribution to the total conversion. According to the literature, the coke level generally increases with the increase in the degree of unsaturation of the fused-ring structure. However, the low coke level of partially hydrogenated compounds (e.g. tetralin) over NaY

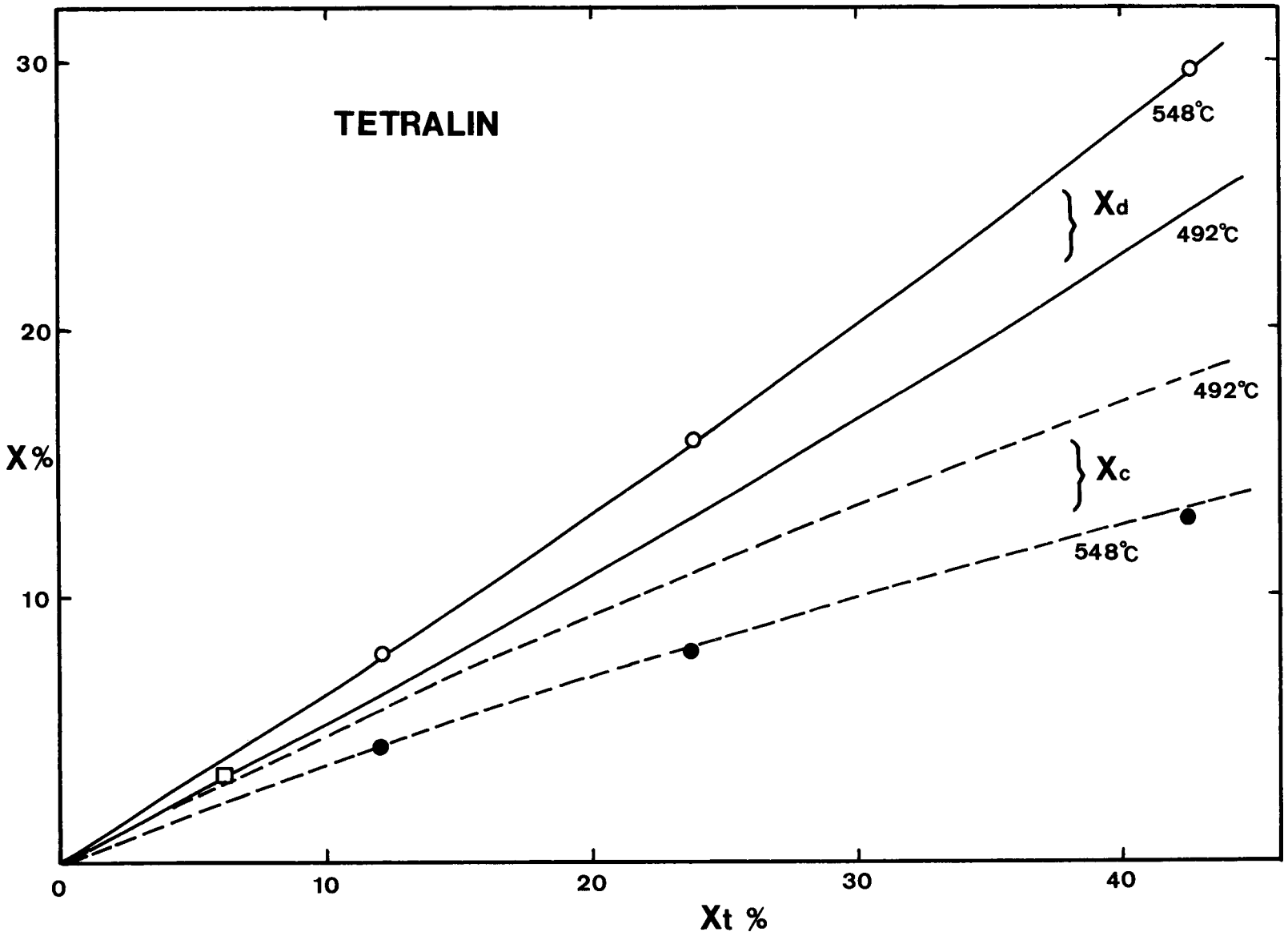

Fig. 6.7. *Selectivity Plot for Tetralin (C_A°, 5.945 Vol % in Vapor at STP).*

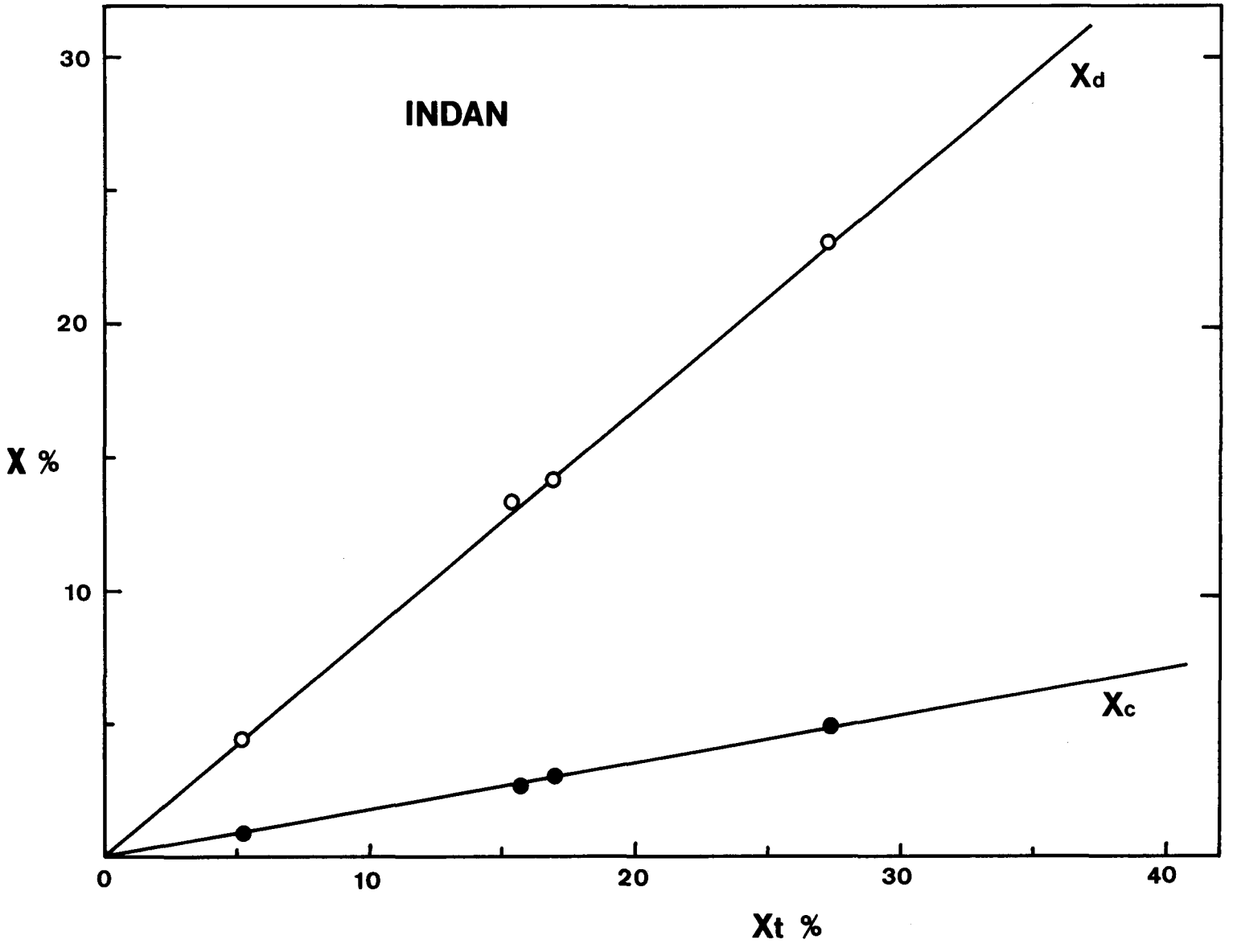

Fig. 6.8. *Selectivity Plot for Indan (C_A°, 6.551 Vol % in Vapor at STP).*

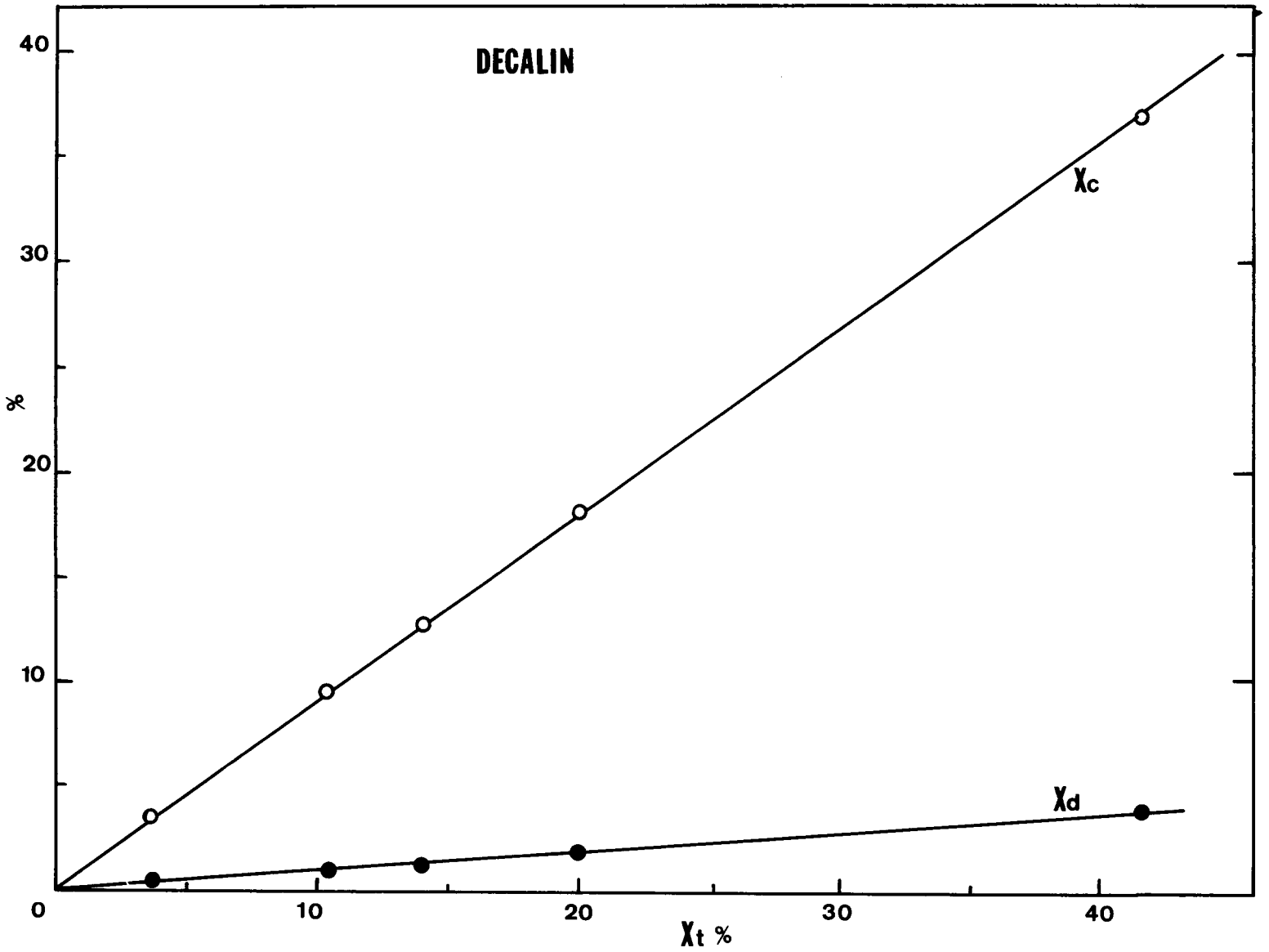

Fig. 6.9. *Selectivity Plot for Decalin (C_A°, 5.216 Vol % in Vapor at STP).*

when compared with that of the saturated compounds (e.g. decalin) as we have seen in Fig. 6.1 may be associated with the high dehydrogenation rate of partially hydrogenated compounds which generates sizable hydrogen to hydrogenate the coke in situ. Figure 6.10 shows the selectivity plot for three-fused ring compounds, octahydrophenanthrene (4.382 vol% in vapor at STP). Because of the higher activation energy for cracking conversion, the cracking products can be enhanced as the temperature increases. However, the dehydrogenation still dominates the product distribution when the total conversion is large.

All the above mentioned selectivity plots are calculated and measured when the initial concentration of reactants are about 5% (vapor phase volume). Therefore, it will be interesting to know the product distribution where no carrier gas is present in the stream (i.e. 100% pure reactant in vapor). Figure 6.11 shows the calculated selectivity plot of the case. It indicates that for saturated fused-ring compounds such as decalin, 1,4 dimethyldecalin, almost 100% of the product results from cracking conversion and for partially hydrogenated fused-ring compounds, dehydrogenation still have 10-30% contribution to the total conversion which depends on the degree of hydrogenation of the fused-ring structure. Experimental verification of Fig. 6.11 is in progress.

In Fig. 6.12, the ordinate is mole % of cracking product excluding the dehydrogenation product. All the measurement for the four compounds of interest are based on a superficial contact time (vol of cat/vol of flow at STP) of four seconds. From the GC/MS analysis, it shows that 45% of the cracked product from tetralin tends to preserve the ring structure to isomerize to methylindan, the other 55% undergoes α-ring opening and then followed by the cracking pattern of n-butylbenzene. In the case of decalin cracking, the cracking product distribution is quite different from that of the partially hydrogenated fused-ring compounds in which toluene, cyclopentane derivatives are present in appreciable amount and also a great amount of gas generated. It is also found that more than 95% of the cracked product from decalin has carbon number less than 9. In the case of octahydrophenanthrene cracking as shown in Fig. 6.13, the cracked product excluding the dehydrogenation conversion shows 30% isomerization product of C_{14} (mainly are naphtha-methylindans), 35% C_{11} and C_{12} (all are tetralin and naphthalene derivatives) product. The C_5-C_{10} range compounds are found only in very small quantity. The reaction product apparently are resulted from the ring opening of the end ring. After end α ring opening, further ring opening seems to be unfavorable. Therefore, it is reasonable to conclude that partially hydrogenated fused ring compounds seem reluctant to crack to small fragments when these compounds are processed over NaY catalyst.

Work Forecast:

In the next quarterly report, the catalytic cracking of partially hydrogenated fused-ring compounds over hydrothermally treated faujasite

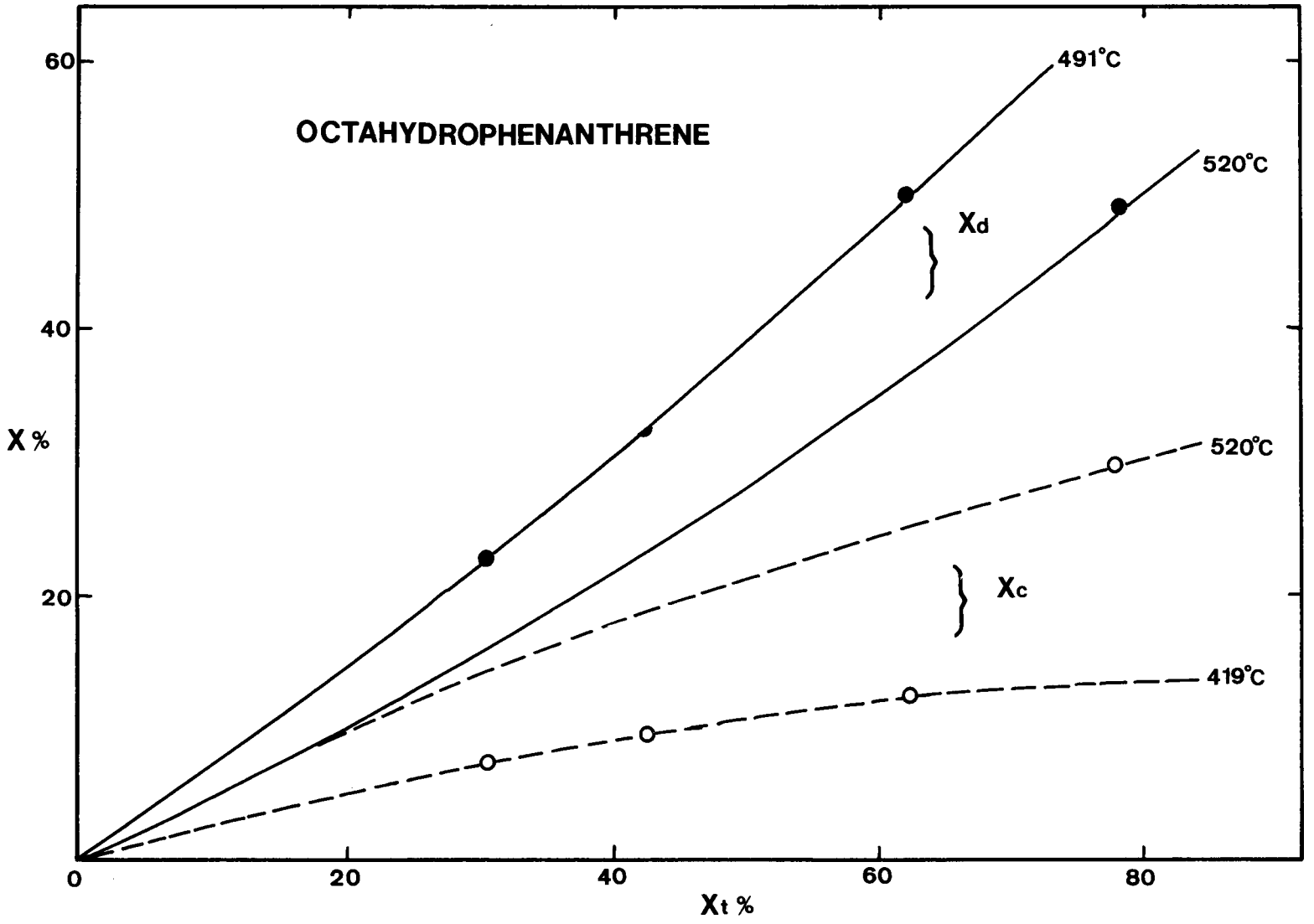

Fig. 6.10. *Selectivity Plot for Octahydrophenanthrene (C_A°, 4.382 Vol % in Vapor at STP).*

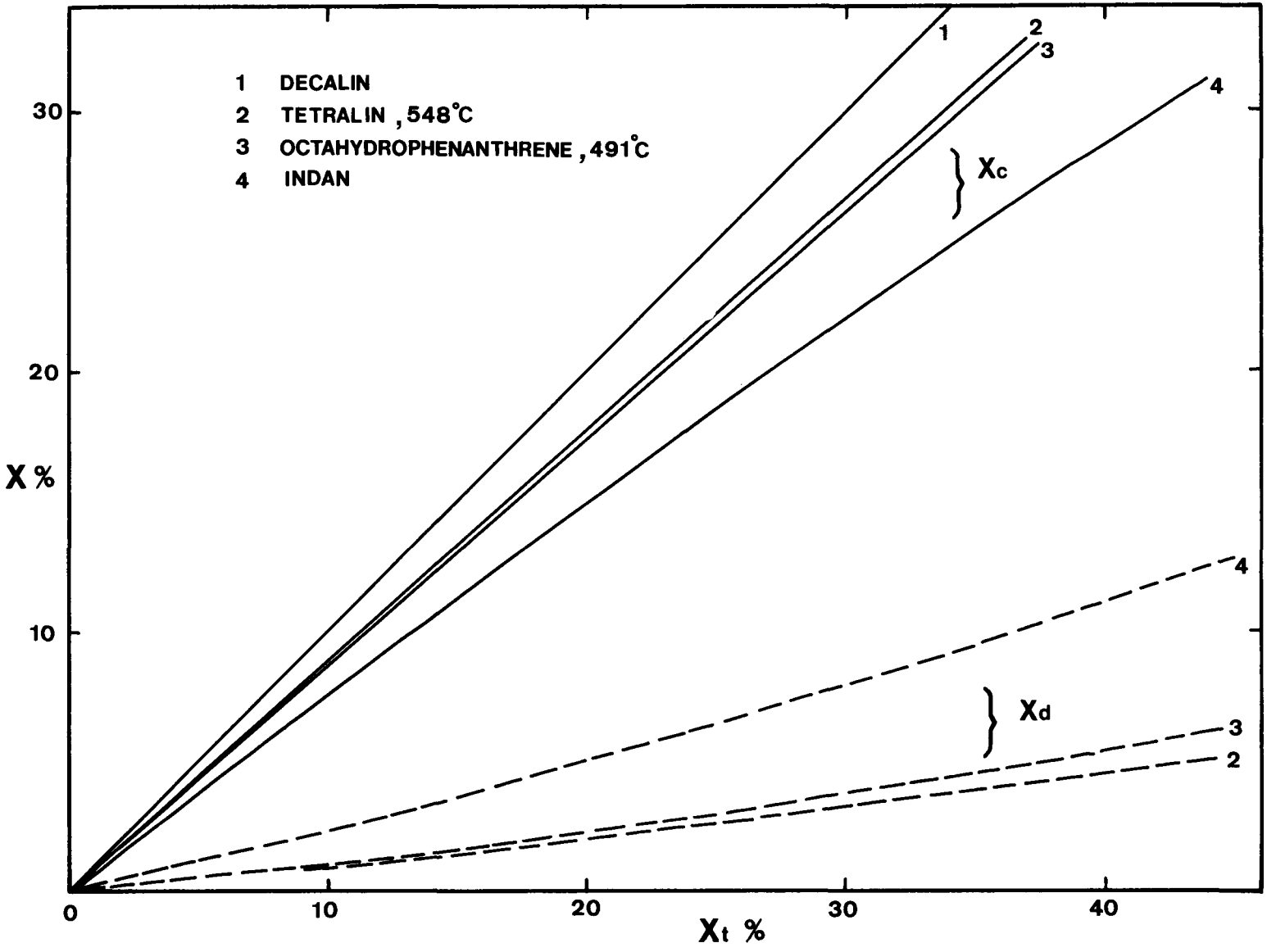

Fig. 6.11. *Theoretical Selectivity Plot (C_A°, 100 Vol % in Vapor).*

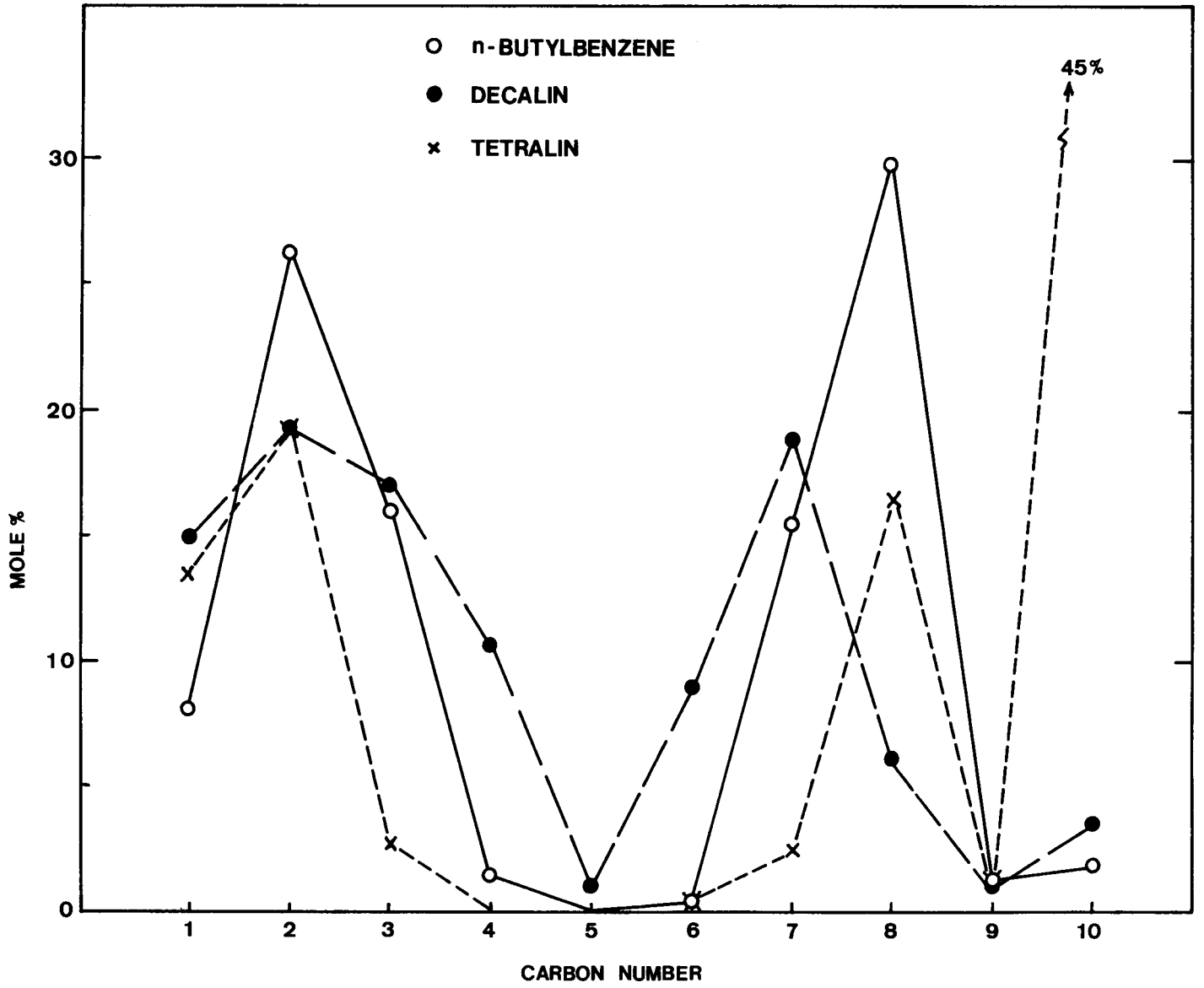

Fig. 6.12. *Carbon Number Distribution from Cracking Conversion (Butylbenzene, 60%, Tetralin, 40%, Decalin 40%). Contact Time, 3.9 seconds.*

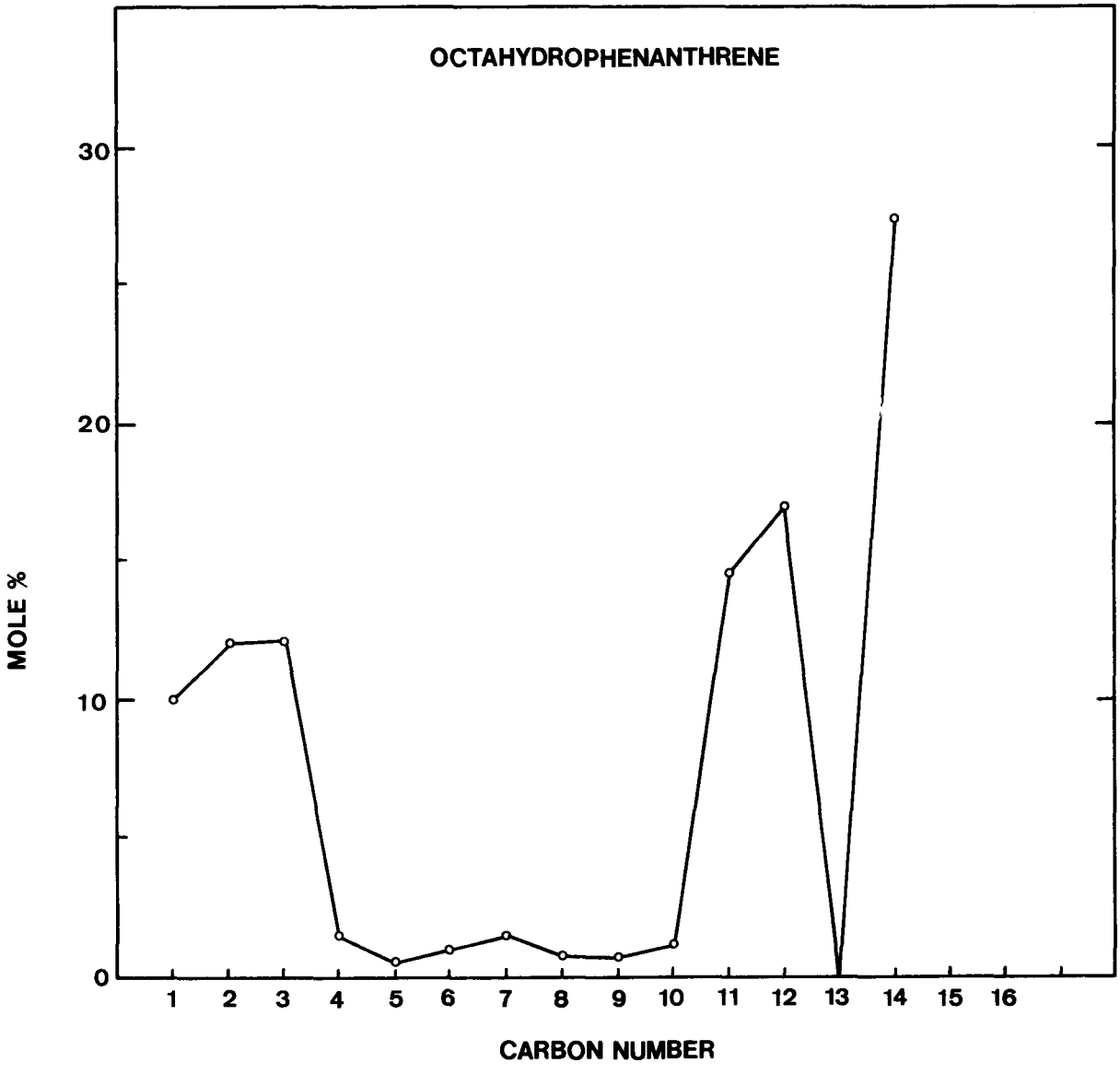

Fig. 6.13. *Carbon Number Distribution from Cracking Conversion for Octahydrophenanthrene at 492°C, Contact Time, 3.9 seconds.*

zeolites (ultra stable Y zeolite) will be detailed. In the next quarter, an effort will be made to run the catalytic cracking experiments under the conditions of absence of carrier gas at higher reaction temperature (~600°C) to investigate the possibility of mass transfer effect.

Task 5 - Hydrocracking Studies on Zeolite-Containing Catalysts - C. Chen, T.M. Lai, and H.W. Haynes, Jr.

During the last quarter a series of catalytic hydrocracking studies was initiated. The catalyst chosen for this investigation is among the most active state-of-the-art zeolite cracking catalysts known. It consists of a hydrothermally stabilized ammonium zeolite Y (ultrastable Y) partially back-exchanged with nickel ion and impregnated with tungsten. The feedstock is a mixture of partially hydrogenated phenanthrenes. Details of the catalyst and feedstock preparations are provided below, but first a brief description of the apparatus will be presented.

Hydrocracking Apparatus

The bench scale hydrocracking unit consists of a tubular flow reactor heated by a Marshall furnace, model 1016, a high pressure syringe pump, Ruska model 2252BI, hydrogen compression facilities, two high pressure accumulators, a wet test meter and a gas collection bag. A schematic is presented in Fig. 6.14. The reactor is a one-half inch heavy wall (0.048") type 316 stainless steel tube packed with catalyst in the central zone (5-6 inches) and 10-20 mesh glass chips in the fore and aft zones. A 1/8" O.D. thermowell extends through the bed and the bed temperature profile can be monitored by means of a movable thermocouple. See Fig. 6.15. The tubular furnace, 20 inches in length, is provided with external connections for shunts which can be used to adjust the temperature profile. An Aminco model J46-13411 compressor maintains the hydrogen feed tank at pressures up to 3000 psi. Hydrogen flow is set by a Whitey No. 22RS4 metering valve and monitored by a differential pressure cell, Barton model 200-41177,connected across a 30 inch capillary 0.009 inches inside diameter. The capillary pressure is held constant at a pressure 250 psi above the reactor pressure by a Tescom model 26-1023-24-002 pressure regulator. The reactor pressure is controlled by a Tescom model 26-1723-24 back pressure regulator. The valving arrangement associated with the high pressure accumulators allows switching from one collector to another without disturbing the system. The exiting gases are vented through a wet test meter and into a polyethylene gas bag. The contents of this bag are analyzed immediately upon completion of an experiment.

Catalyst Preparation

Zeolite catalysts, ion exchanged or otherwise loaded with nickel and tungsten have found wide application as hydrocracking catalysts for petroleum streams. Examples of such preparations abound in the patent literature (e.g. 7-12). As compared with the nobel metal loaded zeolites,

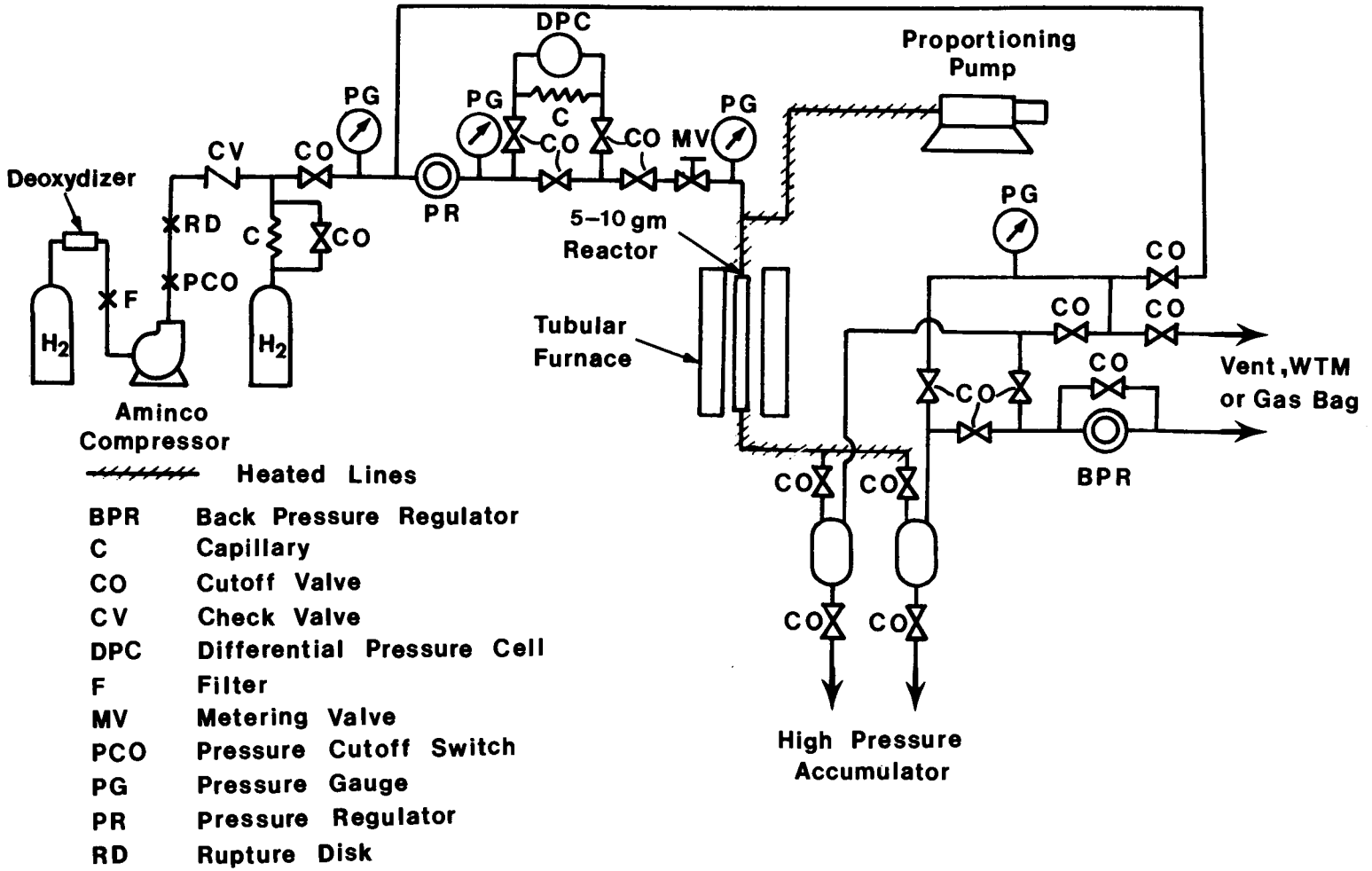

Fig. 6.14. *Bench Scale Hydrocracking Apparatus.*

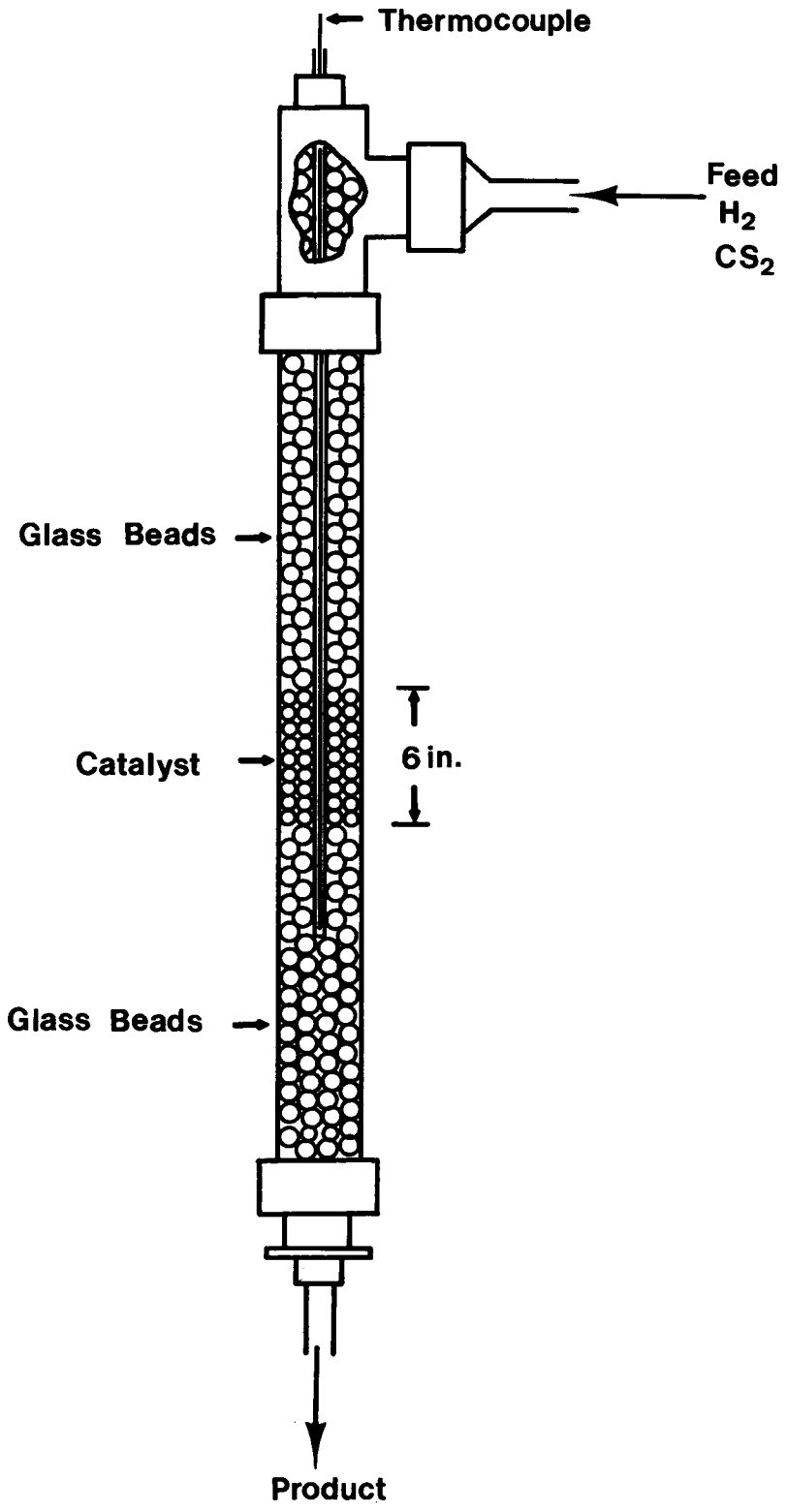

Fig. 6.15. *Reactor Details.*

these nickel-tungsten catalysts possess a much greater resistance to sulfur poisoning. In fact, nickel and tungsten exist as sulfides in the active catalytic state. Several forms of the zeolite base are used in practical applications. Multivalent cation forms, in particular the alkaline earth and rare earth exchanged zeolites possess the activity and stability characteristics required of a practical catalyst. The hydrogen form suffers from stability problems unless the catalyst is subjected to the proper pretreatment conditions. It is known that steaming at elevated temperatures serves to stabilize the zeolite, and under certain specific hydrothermal conditions an extremely active and stable hydrogen form of zeolite Y, an "ultrastable" zeolite Y is formed. One of the authors has recently reviewed zeolite catalyst preparations (13).

The starting point for our catalyst preparation is Linde LZ-Y82 (formerly 33-200) powder. According to company literature LZ-Y82 is an ammonium exchanged form of a thermally stabilized, partially decationized Linde type Y zeolite. The value given for the unit cell size indicates that LZ-Y82 is an ammonium form of ultrastable zeolite Y, i.e. NH_4-USY. The reported composition and properties of the zeolite are reproduced in Table 6.3

The NH_4-USY as received was dried for two hours at 210°C under vacuum and 101.64 gms (dry weight) was slurried in approximately 250 ml distilled water in a 1000 ml beaker. A nickel nitrate solution was prepared by adding 12.5359 gm $Ni(NO_3)_2 \cdot 6H_2O$ (Aldrich-19.7% Ni by analysis) to approximately 250 ml distilled water.

Table 6.3

Composition and Properties of Linde LZ-Y82 Powder*

TYPICAL CHEMICAL PROPERTIES	
SiO_2	72.2 wt.%
Al_2O_3	22.8 wt.%
Na_2O	0.2 wt.%
$(NH_4)_2O$	4.0 wt.%
SiO_2/Al_2O_3, molar ratio	5.38
Na_2O/Al_2O_3, molar ratio	0.01
TYPICAL PHYSICAL PROPERTIES	
LOI at 800°F	23.1 wt.%
Surface Area, 1 pt. B.E.T.	770 m^2/g
Unit Cell Size	24.56 Å

*from company literature

The nickel solution was added slowly to the zeolite slurry with vigorous stirring. After four and one-half hours of stirring at room temperature the slurry was filtered and the filter cake was washed with a total of 500 ml distilled water. The filtrate and washings were collected and analyzed for nickel ion by precipitation with dimethylglyoxime solution (14). The nickel on catalyst was calculated by difference. The filter cake, $NiNH_4$-USY, was dried and ground to a fine powder in a mortor and pestle. Exactly 10.9681 gm of ammonium tungstate, $(NH_4)_2WO_4$, (Aldrich - 69.7 wt.% W by analysis) was dissolved in about 250 ml distilled water. This solution was added to 95.7 gms of the vacuum dried $NiNH_4$-USY in four successive impregnations at incipient wetness. A 9.0485 gm portion of the W-impregnated $NiNH_4$-USY zeolite powder was mixed with 81.10 gms of Conoco Catapal SB (both weights after vacuum drying at 200°C for 2 hrs.) and the powder was tabletted with approximately 0.5 wt.% graphite as a lubricant. The final dry catalyst composition calculated from analysis of the spent nickel solution, recorded weights and the data of Table 6.3 is presented in Table 6.4.

Table 6.4

Calculated Dry Catalyst Composition

$(NH_4)_2WO_4$	1.10wt.%
$NiNH_4$-USY*	8.93 wt.%
$Al_2O_3 \cdot H_2O$	89.96 wt.%

*Ni^{++}/Al mole ratio = 0.042

NH_4^+/Al mole ratio = 0.260

Na^+/Al mole ratio = 0.01

0.312

Prior to charging the reactor, the catalyst was ground and sieved to 10-20 mesh size and calcined in air at 400°C for 16 hours. The catalyst was then charged to the reactor and presulfided with 5% CS_2 in cyclohexane according to the procedure of Table 6.5

Feed Preparation

The hydrocracking feedstock was prepared by hydrogenating pure phenanthrene (Aldrich - 98+%) batchwise in a high pressure autoclave using a supported nickel catalyst (Harshaw Ni-0302T). Several batches were

Table 6.5

Catalyst Sulfiding Procedure

1. Pressure test unit with hydrogen while cold.

2. Pressure unit to 250 psi with hydrogen and set hydrogen flow at 0.25 ℓ(STP)/cc sulfiding feed.

3. Start sulfiding feed (5 wt% CS_2 in CC6) at 2.0 g/hr/gcat. while cold.

4. Raise temperature at a rate of 67°C/hr (2°F/min) to 200°C. Hold these conditions for 2 hours.

5. Raise temperature at rate of 67°C/hr to 300°C. Hold for 1 hour.

6. Cool to ambient temperature with hydrogen and sulfiding feed flowing.

Note: Avoid contacting catalyst with pure hydrogen at elevated temperatures as this will result in reduction to the metal and concomitant losses in activity.

prepared and combined to make a total of about 1700 gms of feedstock. The preparation of a typical batch of feedstock proceeded as follows. Approximately 40 gms of catalyst was reduced in flowing hydrogen at 400°C for 5 hours. After cooling to room temperature the catalyst was submerged in hydrogenated phenanthrenes to prevent direct exposure of the catalyst surface to air. The catalyst and approximately 300 gms of phenanthrene were charged to a one liter stirred autoclave, and after purging the system with hydrogen, the hydrogen pressure was set at 1500 psi (cold). The reactor feed and purge valves were closed and the reactor was heated to a reaction temperature of 300°C. Additional hydrogen was added as needed to maintain a total pressure of approximately 2000 psi. Rough estimates of the hydrogen consumption could be obtained from uptake curves such as the one illustrated in Fig. 6.16.

Analysis of the feed by gas chromatography revealed the feed composition of Table 6.6. The glass column, 2 mm I.D. x 1.9 meters long, was packed with 5% SE-30 on 60/80 mesh Chromosorb P.A.W. Nitrogen carrier flowrate was 25 cc/min. The column oven was temperature programmed at 5°C/min from 50°C initial temperature to 250°C final. The analysis was on a Hewlett-Packard 5840A GC with dual flame ionization detectors. The weight percentages reported in Table 6.6 are in reality area percentages since no FID factors were applied. Identification of the peaks was by gas chromatography-mass spectrometry (Hewlett-Packard 5985). The GC/MS analysis indicated that the peak with retention time 25.15 min is a mixture of dihydrophenanthrene and octahydrophenanthrene isomer. [Other investigators have experienced difficulty in separating these components (15, 16).] With the exception of a small quantity (<1%) of biphenyl, all components of the feed are three-ring species in various states of saturation. We expect that the biphenyl is not a cracked product, but rather a product of hydrodesulfurization of trace quantities of dibenzothiophene impurity in the original phenanthrene. Elemental analysis of the Aldrich phenanthrene yielded 0.23-0.30 wt% sulfur, and a strong smell of hydrogen sulfide was noted when the autoclave was opened at the end of a batch hydrogenation run.

Our reasons for prehydrogenating the hydrocracking feedstock are three-fold. First, the large heat effect which accompanies the hydrogenation of hydrogen-deficient feedstocks is minimized, thus making it possible to more closely approach isothermal conditions in the hydrocracking experiments. Previous studies of phenanthrene hydrocracking from our laboratory were plagued by large temperature gradients within the reactor (17,18,19). Second, the hydrogenated feedstock is a more realistic choice than phenanthrene from the standpoint of commercial hydrocracker operations. Commercial hydrocracker feeds are normally hydrotreated to remove catalyst poisons prior to hydrocracking and some feed hydrogenation is also accomplished. A third reason for hydrogenating the feedstock was to make the feed more pumpable. The mixture of Table 6.6 is a liquid at room temperature, thus the need for cumbersome heated transfer lines is avoided.

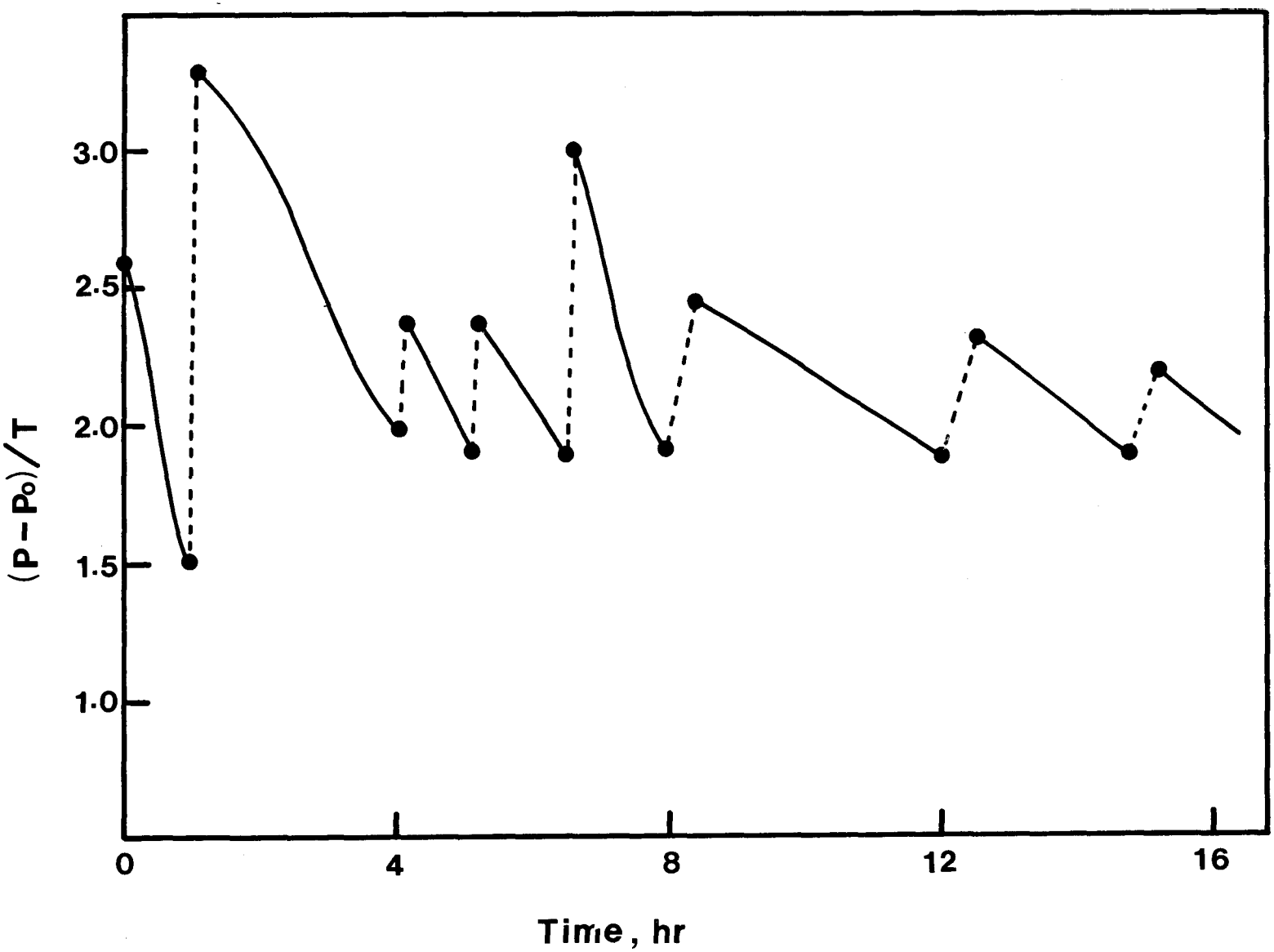

Fig. 6.16. *Hydrogen Uptake Curve for Run BCC-02. Nominal Conditions: P = Total Pressure = 2000 psig, T = Temperature = 573°K, Phenanthrene Charge ≅ 350 g, Catalyst Charge ≅ 33 g, P_o = Phenanthrene Vapor Pressure. Reactor Cooled to Ambient Temperature After 8 hr. of Operation, and Run Resumed on Following Day.*

Table 6.6

Feed Analysis by Gas Chromatography, Run CCC-01

Compound	Weight Percent	Retention Time, mm
Unknown	0.2	16.60
Biphenyl	0.8	17.96
Unknown	0.1	20.29
Perhydrophenanthrene isomer	2.9	20.87
Perhydrophenanthrene isomer	0.9	21.39
Perhydrophenanthrene isomer	1.0	21.99
Perhydrophenanthrene isomer	0.6	22.39
asym-Octahydrophenanthrene isomer	9.9	23.32
Dihydrophenanthrene + octahydrophenanthrene isomer	18.6	25.15
sym-Octahydrophenanthrene	45.6	25.88
Tetrahydrophenanthrene	6.3	26.52
Phenanthrene	13.0	27.00
	99.9	

Experimental

A series of hydrocracking experiments, designated CCC01, was completed during the recent quarter. Nominal run conditions are listed in Table 6.7. In order to maintain the catalyst in a sulfided state, the feed (Table 6.6) was spiked with carbon disulfide to the extent of one weight percent sulfur. The treat gas was pure hydrogen. After completion of the presulfiding procedure, the pump was charged with sulfur spiked feed and the pressure, liquid feedrate and hydrogen rate were set at base conditions. Upon detecting liquid in the product accumulator the furnace was switched on and the temperature was raised slowly (2°F/min, by temperature programming) until the desired base reaction temperature was reached. A minimum of three displacements of reactor volume was allowed prior to each yield period, or balance period, in order to achieve steady-state operation. Base conditions were repeated periodically in order to maintain a check on catalyst activity. At the beginning of a yield period the product was switched to an empty* accumulator and the exit gas line was connected through a wet test meter to a polyethylene gas bag. (See Fig. 6.14.) After processing a minimum of 30 cc of liquid feed, the yield period was terminated by switching to the second accumulator and venting the product accumulator gas through the wet test meter into the gas bag. The liquid product was drained and weighed. In this series of experiments the run duration was 131 hours with no shut-downs. Operability was generally good though some trouble was experienced early in the run with adjustment of the temperature profile. This problem was particularly bad during the 4th yield period, hence the repeat of these conditions in yield period no. 10. Prior to yield period no. 5, the temperature controllor malfunctioned and a temperature excursion to 760°F was experienced. At the completion of yield period no. 13 the reactor was blocked in and cooled under hydrogen pressure to room temperature. The catalyst was still active at the termination of the run as evidenced by the gas analysis, color and viscosity of the liquid product.

Work Forecast:

The liquid products from these experiments will be subjected to elemental and gas chromatographic analyses. Selected products will be analyzed by gas chromatography/mass spectrometry. The data will be analyzed by a computer program which calculates yields, product distributions and material balances. The yields are then adjusted to force a 100 percent carbon material balance. The cracking kinetics will be evaluated in order to make possible comparisons with other systems.

The next system we plan to study is the hydrocracking of hydrogenated pyrenes over a fresh charge of the same NiW-USY catalyst.

---

*The "empty" vessel contained pure hydrogen at system pressure.

Table 6.7

Nominal Run Conditions, Run CCC01.
Hydrocracking of Prehydrogenated Phenanthrene

Run No.	Pressure (Psig)	Temperature (°F)	Space Velocity (gm/hr/gm)	H_2 Rate (SCF/BBL)	
CCC01-1	1500	700	2.0	7500	(Base)
CCC01-2	1500	700	1.0	7500	
CCC01-3	1500	700	0.5	7500	
CCC01-4	1500	700	3.0	5000	
CCC01-5	1500	700	2.0	7500	(Base)
CCC01-6	1500	750	2.0	7500	
CCC01-7	1500	750	1.0	7500	
CCC01-8	1500	650	1.0	7500	
CCC01-9	1500	650	0.5	7500	
CCC01-10	1500	700	3.0	5000	
CCC01-11	1500	700	2.0	7500	(Base)
CCC01-12	2000	700	2.0	7500	
CCC01-13	2000	700	0.5	7500	

References

1. Quarterly Report No. FE-2727-5 for Period October 1 - December 31, 1978, dated February 12, 1978.

2. Ruthven, D.M., ACS Symp. Ser. 40, 320(1977).

3. Cerro, R.L. and Smith, J.M., Ind. Eng. Chem., Fund. 8, 796(1969).

4. Quarterly Report No. FE-2727-4 for Period July 1 - September 30, 1978, dated October 12, 1978.

5. Nace, D.M., Ind. Eng. Chem., Prod. Res. Dev. 8, 24(1969).

6. Nace, D.M., Ind. Eng. Chem., Prod. Res. Dev. 9, 203(1970).

7. Myers, C.G., Rope, B.W. and Garwood, W.E., U.S. Pat. No. 3,384,572, May 21, 1968.

8. Mason, R.B. and Hamner, G.P., U.S. Pat. No. 3,549,518, Dec. 22, 1970.

9. Hammer, G.P. and Mason, R.B., U.S. Pat. No. 3,691,058, Sept. 12, 1972.

10. Buchmann, F.J., Eidt, C.M., Jr., Mason, R.B. and Hamner, G.P., U.S. Pat. No. 3,788,974, Jan. 29, 1974.

11. Ward, J.W., U.S. Pat. No. 3,853,742, Dec. 10, 1974.

12. Bittner, C.W. and Schlaffer, W.G., U.S. Pat. No. 3,959,180, May 25, 1976.

13. Haynes, H.W., Jr., Catal. Rev.-Sci. Eng. 17(2), 273(1978).

14. Pierce, W.C., Sawyer, D.T., and Haenisch, E.L., "Quantitative Analysis," 4th ed., John Wiley, 1958.

15. Skowronski, R.P. and Recht, H.L., Fuel 57, 705(1978).

16. Nakatsuji, Y., Kubo, T., Nomura, M., and Kikkawa, S., Bull. Chem. Soc. Jpn. 51, 618(1978).

17. Wu, W.L. and Haynes, H.W., Jr., ACS Symp. Ser. 20 65(1975).

18. Huang, C.S., Wang, K.C. and Haynes, H.W., Jr., Liquid Fuels from Coal, R.T. Ellington, ed., Academic Press, p. 63-78, 1977.

19. Haynes, H.W., Jr., "The Conversion of Model Coal Liquids Compounds to Naphtha-Species," final rept. to NSF/RANN, Grant No. AER 72-03562, May, 1977.

*U.S. GOVERNMENT PRINTING OFFICE: 1979-640-258-1728